

Comparative Analysis of the Proteomic Profile of Cattle Hides that Produce Loose and Tight Leather using In-Gel Tryptic Digestion followed by LC-MS/MS

by

Catherine Maidment,^{*a} Meekyung Ahn,^a Rafea Naffa,^a Trevor Loo^b and Gillian Norris^{*b}

^a*Leather and Shoe Research Association, Palmerston North 4410;*

^b*School of Fundamental Sciences, Massey University, Palmerston North 4410*

Abstract

Looseness is a defect found in leather that reduces its quality by causing a wrinkly appearance in the finished product, resulting in a reduction in its value. Earlier studies on loose leather using microscopy and Raman spectroscopy reported a change in the collagen structure of loose leather. In this study, proteomics was used to investigate the possible molecular causes of looseness in the raw material, the first time such a study has been carried out. Proteins extracted from two regions of raw hide using two different methods were analysed; those taken from the distal axilla, an area prone to looseness, and those taken from the backbone which is less prone to looseness. Analyses using 1DE-LC-MS/MS showed that although the overall collagen concentration was similar in both areas of the hide, the distribution of the different types of collagen differed. Specifically, concentrations of type I collagen, and the collagen-associated proteoglycan decorin were lower in samples taken from the distal axilla, symptomatic of a collagen network with excess space seen for these samples using confocal microscopy. This study suggests a possible link between the molecular components of raw cattle hide and looseness and more importantly between the molecular components of skin and skin defects. There is therefore potential to develop biomarkers for looseness which will enable early preventative action.

Introduction

Leather is a durable and flexible material that is made by tanning degradable animal skins or hides (by-products of the agricultural industry), to produce a material that is stable and no longer subject to bacterial degradation.¹ The product is classed as high value and is used to make clothing, footwear and furniture.^{1,2} Cattle hide, most commonly used to make leather, is one of the biggest exports in New Zealand, reaching a total of NZD \$353 million annually according to the 2018 Meat Industry Annual Report.³

Looseness is a defect found in cattle hide that causes a wrinkly appearance in the finished leather resulting in reduced leather quality.⁴⁻⁶ Previous studies have investigated looseness in cattle hides using a combination of microscopy,^{4,6} small angle X-ray scattering,⁴ ultrasonic imaging⁵ and Raman spectroscopy⁷ on wet blue or finished

leather samples. In both these studies the hides have undergone a process designed to remove the hair and most of the non-collagenous proteins from the hide involving extremes of pH. Studies by Wood and Wells *et al.*^{4,8} showed there is a larger separation between the fiber bundles in loose leather while Wells *et al.* and Liu *et al.*^{4,6} reported that loose leathers have a gap between the grain and corium layers that is absent in tight leathers. At the molecular level, Mehta *et al.*⁷ detected differences in protein and lipid Raman fingerprints of loose and tight wet blue samples. It is accepted that defects in the hide can result from scarring and insect infestation, careless preparation of hides and skins for tanning such as flay-cuts and gouges, putrefaction, heat damage or poor tanning practices during tanning processing.^{2,9} It is also possible that defects are due to a change in the molecular components of hide caused by poor nutrition, stress, disease or genetic factors.¹⁰

Cattle hide is made up from many different macromolecules. The most abundant of these is protein, with collagen accounting for more than 70% of hide total dry weight.^{11,12} Proteins provide the structural scaffold that makes up hide and is directly responsible for all of its biological functions.¹³⁻¹⁵ Collagen, elastin, proteoglycans and glycoproteins are the predominant proteins in hide, and have a significant and known impact on leather quality.^{1,2} However, due to the rapid advances in mass spectrometry (MS) and proteomic techniques a wide range of other proteins have been identified in low concentrations in animal skins, including that of humans. Such studies have shown that a wide range of proteins are affected by disease, ageing and stress.¹⁶⁻¹⁹

Proteomics is more frequently being used as a tool to identify biomarkers in animals for a range of conditions including infectious diseases such as mastitis, metabolic disorders and the presence of banned compounds in meat and milk.^{20,21} However, to the best of our knowledge only two studies have been published using proteomics to link different molecular components to leather quality.^{22,23} Both of these studies focused on sheepskin rather than cattle hide and no previous publication has used proteomics to investigate potential biomarkers for looseness in cattle hide.

This study used one dimensional gel electrophoresis with liquid chromatography and tandem mass spectrometry (1DE LC-MS/MS) to investigate the proteomic profile of two different regions of raw

*Corresponding authors email: G.Norris@massey.ac.nz or camaidment@hotmail.com
Manuscript submitted May 26, 2020, accepted for publication July 7, 2020.

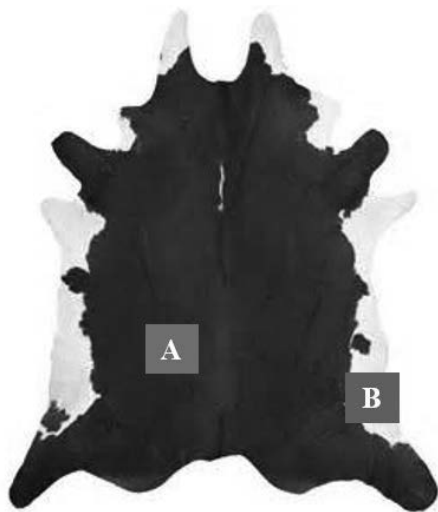


Figure S1. Diagram illustrating the location of the two sampling regions (A) official sampling position (OSP) and (B) distal axilla (DA).

cattle hide; the official sampling position (OSP) which is located near the lower backbone and the distal axilla (DA) which is located in the rear armpit as shown in Figure S1.

These regions have shown variations in mechanical properties,²⁴ such as laxity and extensibility^{24,25} as well as their appearance, pH, temperature, moisture content and microbiome.²⁶ Furthermore, prior studies have shown that the DA region is more prone to looseness than other areas of the hide.⁴

Proteomic studies on the total protein composition of tissues has been traditionally carried out using either gel-based (2D- and 1D-gel LC-MS/MS) or gel-free (1D- and 2D-LC-MS/MS (MudPIT) methods.²⁷ 1D-gel LC-MS/MS was used in this study because it has been shown to enable large-scale analyses of biological systems^{28,29} and was shown to result in a higher number of detected peptides in skin samples in preliminary experiments (results not shown). As hide is known to be very difficult to solubilise,³⁰ two different protein extraction methods were used prior to proteome analysis. One used a traditional lysis buffer whilst the other used a high salt extraction followed by urea extraction.

The discovery of a correlation between the proteomic profile of tight and loose cattle hide will enable a test for defective hides to be

developed as well as adding to the skin proteome bank of knowledge about skin proteins and their changes during development, appearance and disease.

Experimental

Chemicals

All chemicals used for trypsin digestion and analysis were mass spectrometry grade (Optima® LC/MS) chemicals purchased from Fisher Scientific. Exceptions to this include; MS grade Trypsin Gold purchased from Promega; Wisconsin, USA, cOmplete® protease inhibitor tablets from Roche Diagnostics; Mannheim, Germany. DL-Dithiothreitol (DTT) from Gold Biotechnology; USA and iodoacetamide, urea and thiourea from GE Healthcare; Buckinghamshire, UK. Coomassie blue G-250 and 3-[(3-cholamidopropyl) dimethylammonio]-1-propanesulfonate (CHAPS) from Biorad; California USA. The following chemicals were purchased from Sigma Aldrich; St. Louis, USA; glass beads (acid washed) and norleucine and stock amino acid standard solution containing 2.5mM of each amino acid except proline and hydroxyproline at 12.5mM and cystine at 1.2mM. 6-Aminoquinolylcarbonyl (AQC) from Synchem, Germany. All other chemicals were analytical grade.

Sample Preparation

Four raw hides obtained from Tasman Tannery; Whanganui, NZ were cut in half and 3 samples cut from the OSP and DA region of one half of each hide, then stored at -20°C for later analysis. The other half of the hide was processed to finished leather using conventional methods.⁴ Looseness was measured using the SATRA STD 174 break/pipiness scale (SATRA Technology; Northamptonshire, UK) which consists of a graded selection of leather replicas numbered one to eight with one having the least severe wrinkles and eight having the most severe.

Protein extraction

Raw hide samples were shaved to remove the hair, then cut into approximately 1 cm² blocks. These were sliced into 10µm thick sections using the Leica CM 1850 UV cryostat (Leica Biosystems; Wetzlar, Germany) and approximately 50mg of grain, grain to corium junction and corium layers were collected as shown in Figure S2.

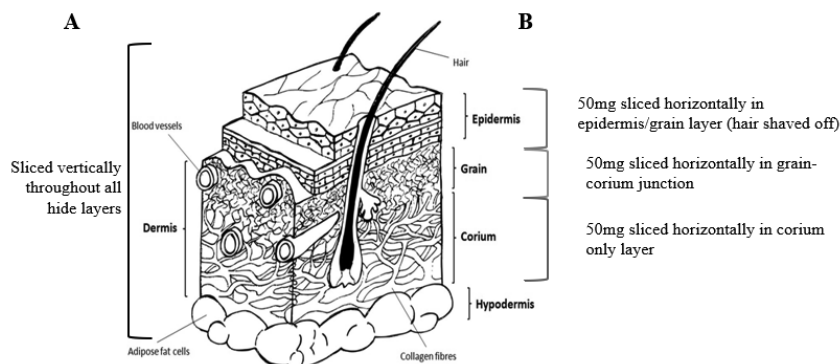


Figure S2. Diagram of how the hide was sliced (A) for confocal microscopy images (60µM thick slices) and (B) for protein extraction (10µM thick slices).

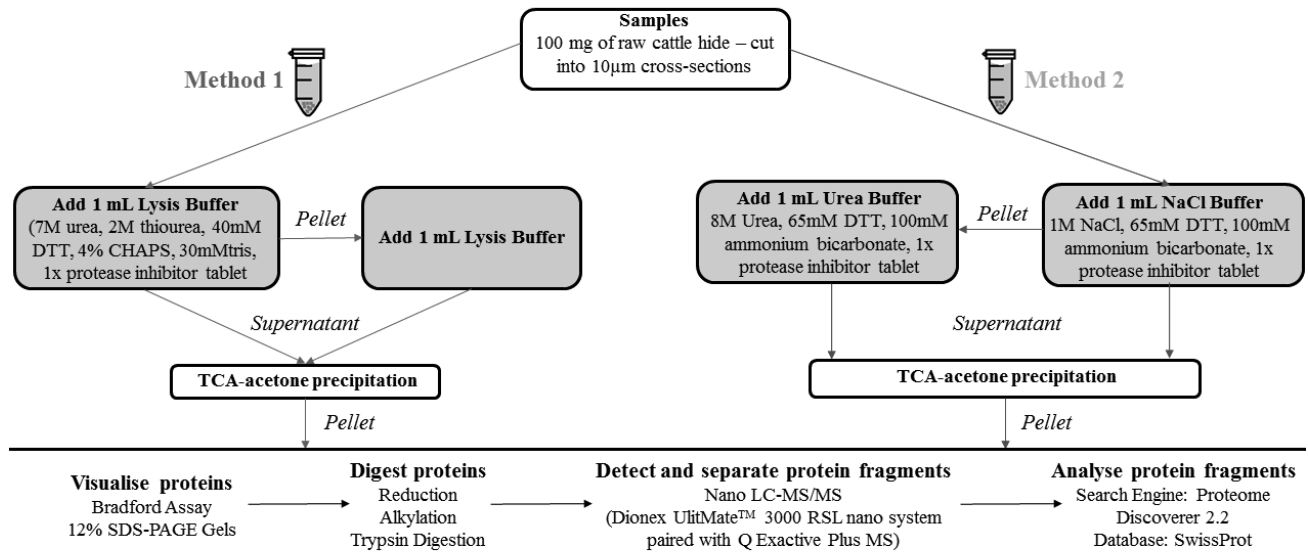


Figure 1. Flow diagram of protein extraction from cattle hide samples followed by in-gel tryptic digestion and LC-MS/MS analysis.

The samples were placed in 1.5 mL Eppendorf tubes then immersed in extraction buffer; either Lysis (7M Urea, 2M thiourea, 40mM DTT, 4% CHAPS, 30mM tris and 1x cOmplete® protease inhibitor tablet used according to the manufacturer's instructions, pH 7-9) or NaCl (1M NaCl, 65mM DTT, 100mM ammonium bicarbonate and 1x cOmplete® protease inhibitor tablet, pH 8) for 24 hours at 4°C. The extraction was aided by mechanical action provided through adding glass beads to each tube which was then placed on a rotating wheel (LABNET, USA) overnight. After this time, residual hide was removed from the protein solution by centrifugation at 16,500 x g for 30 minutes. The pellet was then treated with a second lot of extraction buffer either a repeat of lysis buffer or Urea buffer (8M Urea, 65mM DTT, 100mM ammonium bicarbonate and 1x cOmplete® protease inhibitor, pH 8) as shown in Figure 1. The supernatants from both lysis buffer extractions were pooled as were the supernatants from the sequential extraction and the proteins precipitated by the addition of 25% TCA in acetone in a (v/v) ratio of 1:9. After incubation at -20°C for at least 2 hours precipitated proteins were pelleted by centrifugation at 5,000 x g for 20 minutes, and the resulting pellets washed 3 times in cold acetone before being resuspended in the minimum volume of sample solution (7M Urea, 2M thiourea, 40mM DTT, 4% CHAPS and 1x cOmplete® protease inhibitor tablet, pH 7-9).

Protein digestion

The concentrations of the samples were measured using the standard Bradford assay protocol.³¹ An equal volume of sample was mixed with the same volume of sample loading buffer (10% (v/v) SDS, 50% (v/v) glycerol, 100mM DTT, 0.25M Tris-HCL, 0.05% (w/v) bromophenol blue) and run on 12% Tris-glycine SDS-PAGE gels at 150V for approximately 90 minutes alongside precision plus protein™ dual xtra standards ranging in molecular weight from 250kDa to 20kDa from BioRad. Following electrophoresis, the gels were fixed in ethanol: acetic acid (40:10 (v/v)) for 15 minutes before being stained overnight with Colloidal Coomassie brilliant blue G250.³²

Each lane was manually cut out of the gel using a sterilised scalpel blade then sliced into 6 even pieces (Figure S3). After cutting each band into small pieces, they were destained using 50% methanol, 5% acetic acid and dehydrated in 200µL acetonitrile. The gel pieces were air dried before being reduced by the addition of 50µL of 10mM DTT in 100mM ammonium bicarbonate. After 1 hour at room temperature, the solution was removed and replaced with 50µL of 200mM iodoacetamide in 100mM ammonium bicarbonate and the tubes incubated for 1 hour at room temperature in the dark. After this time the alkylating solution was removed, and the gel pieces washed in acetonitrile and dehydrated as before. They were then rehydrated and subjected to in-gel digestion with 6 µL 100µg/mL MS grade Trypsin Gold in 50 µL ammonium bicarbonate, 1mM CaCl₂, 10% (v/v) acetonitrile at 37°C overnight. The supernatant was carefully removed from the gel pieces and placed in a Lo-Bind Eppendorf tube. Any trapped peptides were extracted from the gel pieces by sonication in 40µL 50% (v/v) acetonitrile, 5% (v/v) formic acid. The resulting supernatant was added to the first before being concentrated to a final volume of 20µL using vacuum centrifugation.³³

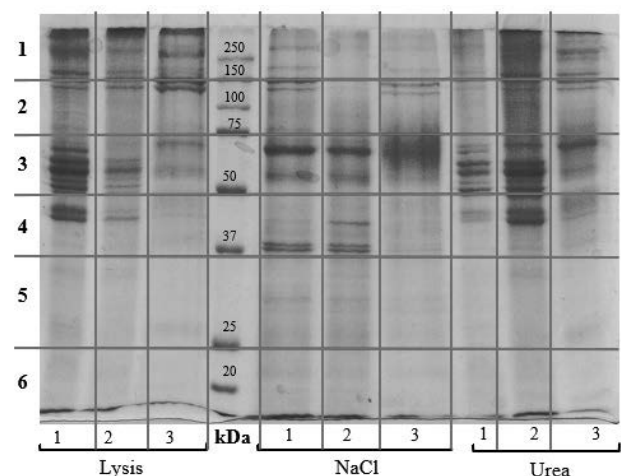


Figure S3. Diagram of how the SDS-PAGE gels were manually cut.

LC-MS/MS analysis

2 µl of each sample (4 biological replicates with 3 technical replicates each) were injected on a 1.0 mm × 5 mm PepMap 100 C₁₈ trap column, 5 µm particle size, at a flow rate of 25 µl/min then onto a 75 µm × 50 cm PepMap C₁₈ column, 3 µm particle size, at a flow rate of 300 nL/min using a Dionex Ultimate™ 3000 RSL nano system (Thermo Fisher Scientific, Massachusetts, USA). The mobile phase was 3% acetonitrile, 0.1% formic acid in MS grade H₂O. Peptides were eluted using a linear gradient from 3-30% acetonitrile, 0.1% formic acid over 55 minutes. The peptides eluted from the column were analysed using a Q Exactive Plus mass spectrometer with a Nano Flex ionization source operating with Xcalibur acquisition software (Thermo Fisher Scientific, Massachusetts, USA). The mass spectrometer was externally calibrated and operated in data-dependent mode. Full MS1 scans were acquired over a mass range of 375-1,500 m/z with a resolution setting of 70,000, while fragment ion spectra were acquired at a resolution of 17,500. For data dependent acquisition of HCD spectra, the top ten most intense ions were selected for fragmentation in each scan cycle and full MS and fragment ion spectra were detected by the Orbitrap mass analyser. Exclusion conditions were optimised according to the observed peak width (typically 10s).

Protein Identification

Processing of the raw data generated from LC-MS/MS analysis was carried out using Proteome Discoverer version 2.2 (Thermo Fisher Scientific; Massachusetts, USA). For the analysis, the grain, grain-corium junction and corium data from each extraction were combined. The following search parameters were used for protein identification: peptide mass tolerance 10 ppm, MS/MS mass tolerance 0.02 Da, up to two missed cleavages allowed, minimum peptide length, six amino acids, carbamidomethylation of cysteine was set as a fixed modification and oxidation of methionine, lysine and proline, acetylation of the N-terminal residue, and galactosyl, glucosylgalactosyl modifications of lysine were set as variable modifications. For each protein, the minimal number of unique peptides identified was set to two and the false discovery rate was set at 1%. The number of proteins initially identified was reduced from over 10,000 to approximately 1,000 using these criteria. Data were searched against the UniProtKB-SwissProt database (taxonomy: Bovine, release 10/2016).

Statistical analysis

Analysis of each sample was performed in three separate experiments. Statistical differences between the groups OSP and DA were determined using one-way student *t*-tests and volcano plots. In order to be classified as significantly different the *p*-value had to be less than 0.05 and the fold change greater than 2. Data analysis *via* principal component analysis (PCA) plots and visualization *via* heatmaps was carried out using the publicly available MetaboAnalyst 4.0 software (<https://www.metaboanalyst.ca/>).

Total collagen concentration

Total collagen concentration in the OSP and DA samples was analysed based on a method previously reported by Naffa *et al.*^{11, 12}

with slight modifications. 100 mg of lyophilized 40 µm slices of each skin sample were hydrolysed in 5 ml of 6 M HCl containing 3% (w/v) phenol for 24 hours at 110°C. The hydrolysate was filtered, concentrated by lyophilisation then dissolved in 1.0 ml of 0.1 M HCl, it was then diluted 1:100 with MilliQ H₂O before being derivatized with AQC (10 µl sample, 100 pmol/µl norleucine, 15 pmol/µl AQC in 0.2 M borate buffer, pH 8.85) for 10 minutes at 55°C. After a further 1:10 dilution, 1 µl of sample or 1-5 µl of amino acid standard were injected on to a 150 × 4.6 mm Gemini C₁₈, 5 µm HPLC column (Phenomenex; California, USA). Solvent A was 5 mM ammonium acetate, 1% acetic acid, pH 5.05 A and solvent B was 60% (v/v) acetonitrile in water. Solute was eluted using gradient elution (0-100% B), over 90 minutes at a flow rate of 1.00 ml/min and a column temperature of 37°C. Eluted peaks were separated and monitored using a Dionex UltiMate™ HPG-3400RS rapid separation binary pump with fluorescence detector (Dionex RF 2000). The excitation and emission wavelengths were set at 245 nm and 395 nm respectively. Amino acid concentrations were determined using calibration curves calculated using Dionex CHROMELION version 6.80 SR13 Build 3967.

3D Confocal Microscopy

Picrosirius red was used to stain the collagen network, using the slightly modified method of Naffa *et al.*¹¹ Briefly, 2 × 2 cm hide samples were fixed in buffered formalin (40% formaldehyde, 30mM di-sodium hydrogen orthophosphate and 30mM sodium dihydrogen orthophosphate, pH 7.4) for 24 hours before being sliced into 40 µm thick cross sections using the Leica CM 1850 UV cryostat. The slices were carefully placed on microscope slides then rinsed with H₂O, before being placed in a 1% (w/v) potassium permanganate solution for 5 minutes. They were then rewashed with H₂O, before being placed in a 1% (w/v) oxalic acid solution until they became colourless. After washing in H₂O, they were placed in 0.2% (w/v) phosphomolybdic acid for 10 minutes, then stained with 1.2% (w/v) picric acid containing 0.1g sirius red F3B for 60 minutes. After this time, the slides were placed in 0.01 N HCl for 15 minutes, washed with ethanol then placed in xylene (100%). Coverslips were attached using DPX containing dibutyl phthalate (10-20%) and xylene (100%) as the mounting solution.

A Leica SP5 DM6000B scanning Confocal Microscope with LAS AF software (version 2.7.1.9723) was used to visualize the collagen network using the parameters previously published by Vogel *et al.*³⁴ Images were acquired using a 20× lens with a 3× optical zoom and standard filters set at an excitation and emission wavelengths of 561 nm and 571 - 653 nm respectively.

Results and discussion

Proteomic profiles: A comparison of the extraction methods

A wide range of methods have been reported for protein extraction from different tissues, including hide.^{30, 35-37} Efficient extraction of protein from hide is difficult because by its very nature, hide has limited solubility, thus it is common to use a combination of mechanical and

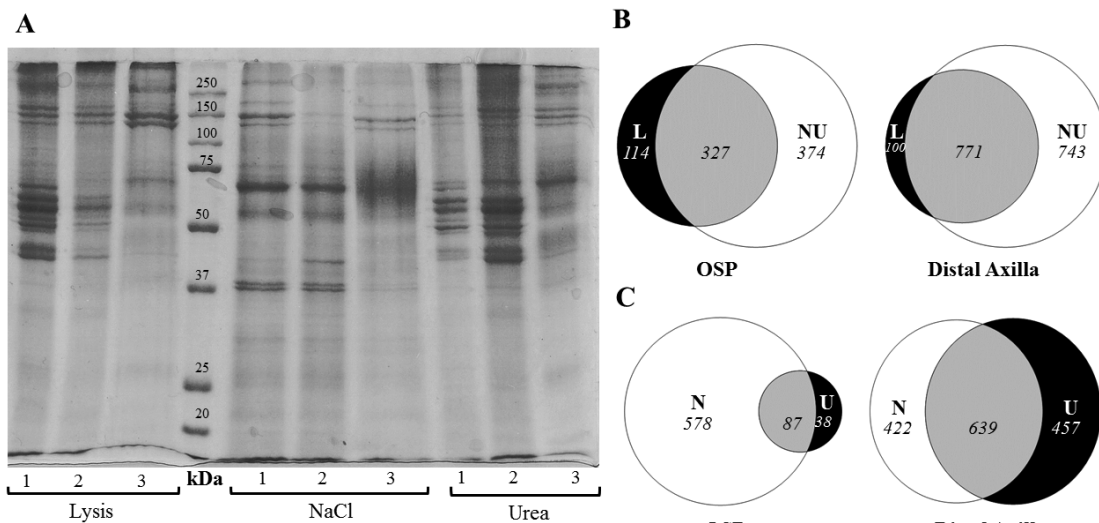


Figure 2. Proteomic profiles of cattle hide using different extraction methods. **A)** SDS-PAGE gel of proteins extracted from cattle hide using lysis, NaCl and Urea extraction buffers (1-grain, 2-grain-corium junction and 3-corium). **B)** Venn diagrams illustrating the number of proteins identified via the lysis (L) and NaCl/Urea (NU) extraction methods in both the OSP and DA regions. **C)** Venn diagrams illustrating the number of proteins identified individually by the NaCl (N) and urea (U) sequential extraction method in both the OSP and DA regions.

chemical methods.³⁰ This study used glass beads with rotation to provide mechanical action followed by sequential extraction with two different extraction buffers to investigate which was more effective.

Method 1 (Fig 1) used a traditional lysis buffer containing urea/thiourea to denature the proteins, a reducing agent (DTT) to reduce disulfide bonds, the detergent CHAPs for solubilisation of poorly soluble proteins and a protease inhibitor (cOmplete) to control undesirable proteolysis in a Tris buffer system, pH 7-9. Method 2 (Fig 1) used a high salt (NaCl) buffer followed by a buffer containing a high concentration of urea. NaCl is known to increase the concentration of extracted proteins as well as the number of higher molecular protein bands such as collagen³⁸ and contained a reducing agent and protease inhibitor in ammonium bicarbonate buffer (pH 8). The urea buffer contained a relatively high concentration of urea, known to efficiently denature and solubilise proteins, a reducing agent (DTT) and protease inhibitor (cOmplete) in an ammonium bicarbonate buffer. What was not done in this study was to use more than one protease to produce a greater coverage of the proteome as has been done in other studies,³⁹ however despite stringent filters over 400 proteins were identified with high confidence.

The protein profile of samples extracted using the lysis extraction buffer and the sequential NaCl/urea methods were different as shown by SDS-PAGE (Fig 2a) with the sequential method producing a greater number of bands. Not surprisingly, there were a greater number of proteins identified from this extraction by LC-MS/MS (Fig 2b). When comparing the proteins extracted from the individual steps of the sequential extraction, very different protein bands were seen on the gel. This was especially apparent in the OSP where only 87 proteins were common to the NaCl and urea extraction (Fig 2c). On the other hand, proteins extracted using

the lysis buffer and the urea buffer had similar banding patterns on the gel. Although the sequential NaCl/Urea buffer extracted a greater number of proteins compared to the lysis buffer there were still a significant number of proteins unique to the lysis extraction suggesting that combining different fractionation and extraction methods results in a more complete proteome coverage. In all three extraction methods differences in banding pattern were observed between the three different layers with the grain having the most diverse banding pattern and the corium the least. This is most likely due to the corium being more collagen rich whilst the grain had more non-collagenous proteins. These layers were combined when analysing the mass spectrometry data.

Differences between the OSP and DA regions of raw cattle hide

The looseness grade of the OSP and DA regions from the half cattle hides processed to leather were analysed using the SATRA break scale. On average, the DA was significantly looser than the

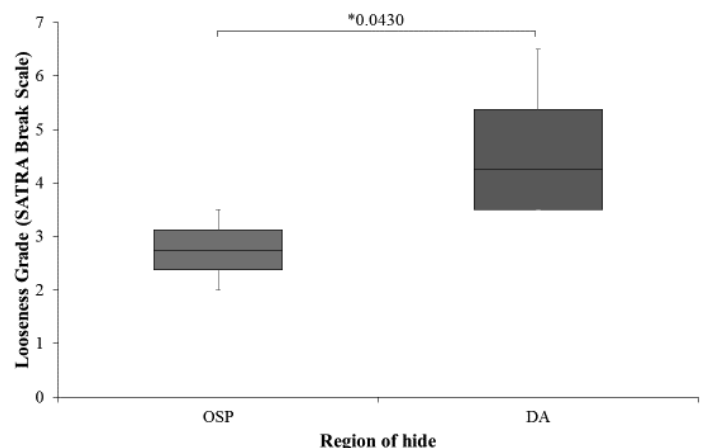


Figure 3. Looseness grade of OSP and DA region of leather samples, * p-value.

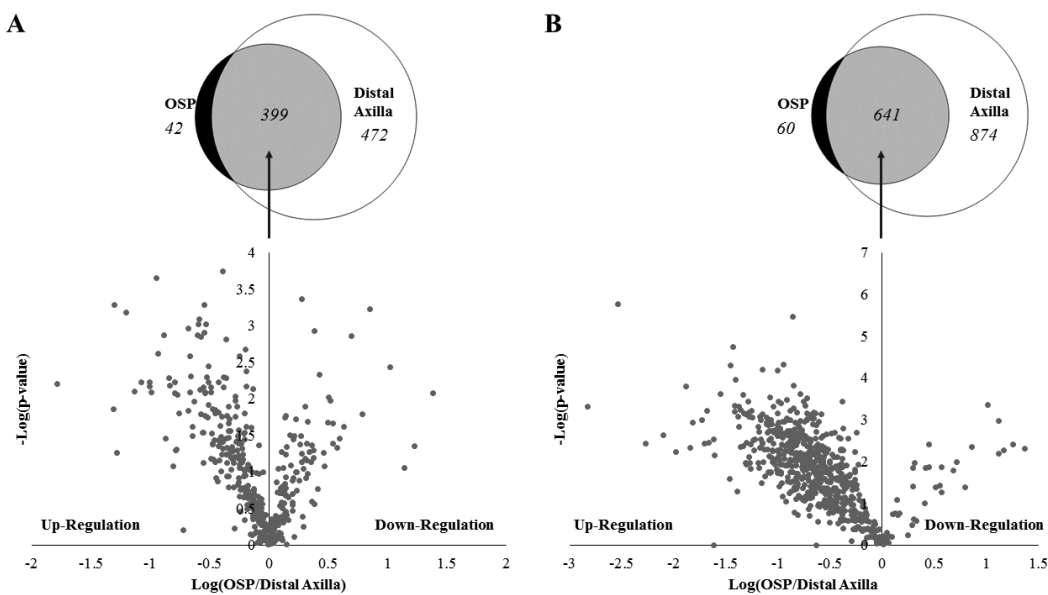


Figure 4. Venn diagrams comparing the number of proteins identified in OSP and DA samples and volcano plots comparing the statistical significance vs fold change in the abundance of proteins found in the OSP and DA for A) lysis extraction and B) sequential NaCl/Urea extraction.

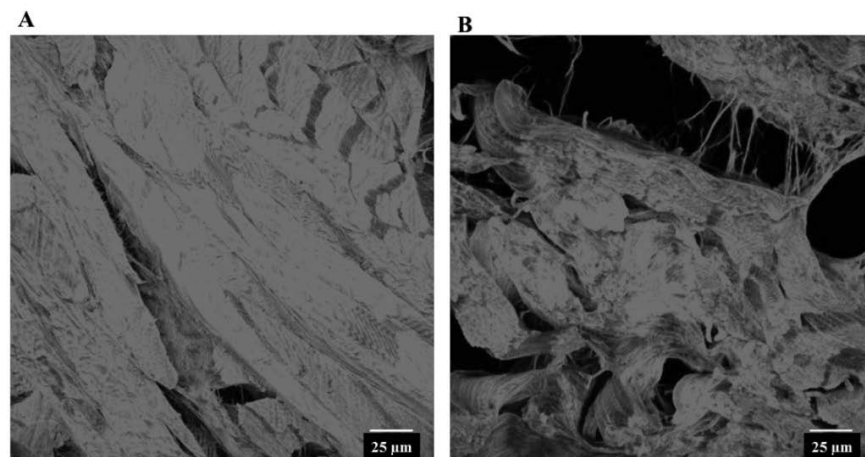


Figure 5. 3D confocal microscopy images of A) OSP region and B) distal axilla region of cattle hide.

OSP region (p-value 0.0430) for the four hides tested (Fig 3). This is consistent with previous reports by Wells *et al.*⁴ and Mehta *et al.*⁷ which state that the DA region is more prone to looseness in cattle hide. The proteomic profiles of the OSP and DA regions from the raw hide half were then analysed using in-gel LC-MS/MS.

Proteomic analyses identified 439 proteins with high confidence from the lysis extraction and 701 proteins with high confidence from the NaCl/urea extraction for samples taken from the OSP region. Samples from the DA region yielded 868 identifications using lysis buffer extraction and 1515 proteins extracted using NaCl/Urea (Fig 4). Interestingly, the proteins that were common to both the OSP and DA regions were typically up-regulated in the OSP region suggesting that regardless of the more complete extraction of proteins from the DA region there are higher concentrations of these proteins in the OSP region compared to the DA as shown in Fig 4.

The greater number of proteins identified in the DA region is potentially due to the increased space between the collagen fibers that is seen using confocal microscopy (Fig 5) and has been reported by others.^{4,8} A looser arrangement of fiber bundles would enable easier access of the solubilisation reagents to the protein fiber network, resulting in an increased number of proteins extracted. The fact that similar observations were made both in this study and other studies^{4,8} suggests that the large gaps seen between the fiber bundles in loose leather are present in the raw material and are not caused by poor tanning practices.

PCA plots analysing all data (Fig 6) and heat maps containing the 50 most abundant proteins (Fig 7) were used to display the overall results of LC-MS/MS data. The PCA plots show distinct clustering of groups of proteins from the OSP and DA samples (Fig 6), strongly

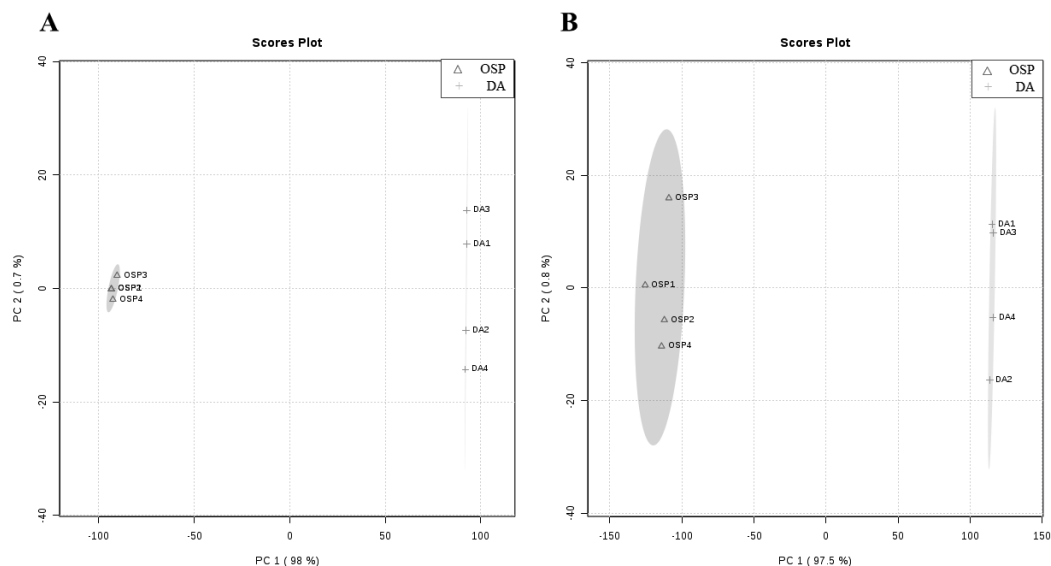


Figure 6. 2D score plots of four OSP and DA region samples for **A)** Lysis extraction and **B)** NaCl/urea extraction based on two principal components.

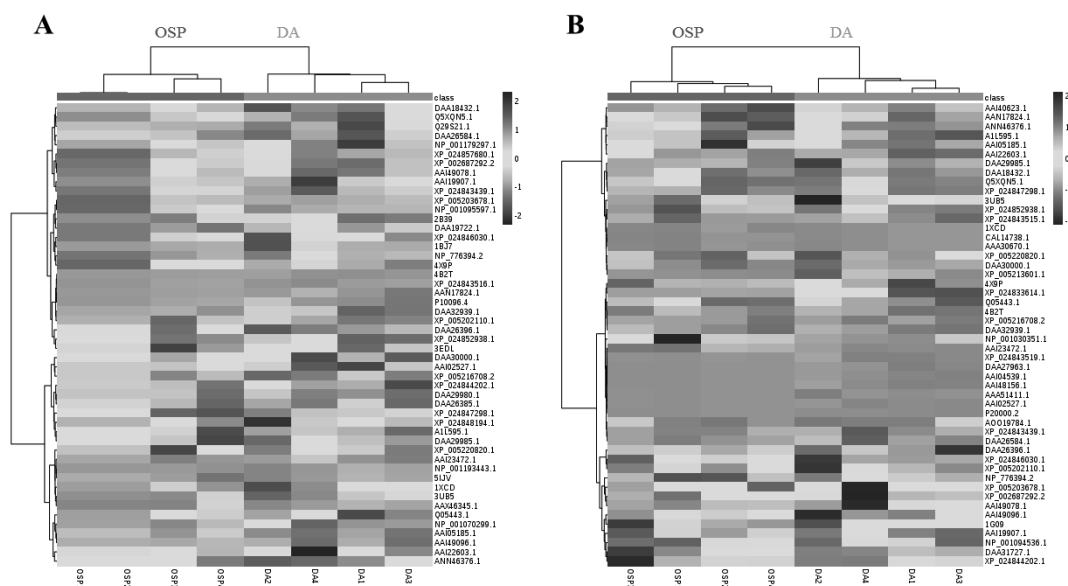


Figure 7. Heat maps of 50 most abundant proteins as identified by accession number from **A)** Lysis extraction and **B)** NaCl/urea extraction.

suggestive of a real difference in the protein composition between the DA and the OSP regions of the hide. The heat map supports this finding, showing significant differences between the relative concentrations of some protein groups in the DA and the OSP samples (Fig 7).

All proteins that were common to both the OSP and DA region (399 and 641 for the Lysis and NaCl/Urea extractions respectively) were analysed to determine whether there were any significant differences between the relative concentrations in the two regions. In order to be categorised as significantly different the proteins had to have p-values below 0.05 and a fold change equal to or greater than 2. Only 38 proteins met these constraints and all were down-regulated in the DA samples. Proteins included fibrous collagen, proteoglycans

and other ECM proteins, keratins, cellular proteins, enzymes and serum proteins and are listed in Table I.

Fibrous collagens type I and III are down-regulated in DA samples. Fibrous collagen is the most abundant collagen in hide and provides mechanical and structural support to the hide with type I being more prevalent in the corium and type III in the grain.^{40,41} A decrease in the fibrous collagen may result in a less organised collagen network, as seen in figure 5, which could contribute to the development of looseness. However, the overall collagen content of OSP and DA samples was not significantly different when calculated using the hydroxyproline concentration measured by amino acid analysis⁴² (Fig. 8). Because LC-MS/MS measures only the soluble protein in contrast to amino acid analysis which measures both soluble and

insoluble collagen, this is not entirely unexpected. Further validation steps are needed to confirm whether fibrous collagen is indeed down-regulated in the DA region, using immunological detection.

The proteoglycan decorin and proteoglycan associated protein glial hyaluronate binding protein are also down-regulated in DA samples. The core protein of decorin interacts with specific surface amino acid residues on type I collagen fibrils, the interaction being stabilised by electrostatic interactions between collagen and the sulfates of the GAG.⁴³ This interaction is necessary for assembly of collagen microfibrils and prevents the cleavage of collagen fibrils by matrix

metalloprotease I.⁴³ As such, lower concentrations could affect collagen fiber bundle architecture. The glial hyaluronate binding protein is believed to be a proteolytic product of versican.⁴⁴ Versican is a hyalectan that binds to both hyaluronic acid and lectins and has roles in regulation of cell adhesion, migration and proliferation, ECM assembly and fibrillogenesis of elastic fibers.⁴⁵

As seen in Table I many keratins were down-regulated in the OSP compared to the DA. As keratins are removed during the dehairing stage of leather processing it is unlikely that they contribute to looseness. It is therefore possible that the difference in the

Table I
Proteins that are significantly down regulated in the DA

	Protein	Accession	p-value	OSP/DA	Extraction Method	
<i>Fibrous Collagen</i>	Collagen type I: alpha 1	AAI05185.1	0.0396	1.99	NU	
	Collagen type I: alpha1 CN8	0910139A	0.0474	3.77	L	
	Precursor of collagen type III: alpha-1	NP_001070299.1	0.0213	3.15	L	
<i>Proteoglycans and ECM proteins</i>	A Chain A, Decorin	1XCD	0.0204	2.11	L	
	Glial hyaluronate-binding protein	AAB20399.1	0.0381	3.61	NU	
<i>Keratin</i>	Keratin 31	DAA18488.1	0.0239	4.27	L	
	Keratin 82	DAA29986.1	0.0216	3.46	L	
	Keratin 84	DAA29999.1	0.0409	3.46	L	
	Keratin 86	DAA30000.1	0.0144	1.98	NU	
	Keratin 83	AAI23472.1	0.0037	10.54	L	
	Keratin I: cytoskeletal 27	DAA18462.1	0.0006	7.10	L	
	Keratin I: cytoskeletal 39	XP_010814574.2	0.0083	24.44	L	
	<i>Cellular proteins</i>	A Chain A, Actin, Cytoplasmic 1	3UB5	0.0047	2.67	L
		Actin, gamma-enteric smooth muscle	NP_001013610.1	0.0147	2.64	NU
Annexin I		AAB25084.1	0.0441	16.87	L	
			0.0412	3.31	NU	
Histone H2B type 1-K		DAA16155.1	0.0014	5.00	L	
Myosin-11		NP_001095597.1	0.0065	13.23	NU	
Isoform X1 of Periostin		XP_005213601.1	0.0045	7.29	NU	
Isoform X13 of Tropomyosin alpha-1 chain		XP_024853024.1	0.0164	4.89	NU	
Isoform X3 of Tropomyosin beta chain		XP_005210126.1	0.0138	3.77	NU	
Tubulin alpha 1C chain-like		XP_024838025.1	0.0049	23.66	NU	
Tubulin alpha 4a		AAI18200.1	0.0138	2.82	NU	
Tubulin beta 4B chain		NP_001029835.1	0.0011	13.34	NU	
Isoform X1 of V-set and immunoglobulin domain-containing protein 8		XP_010801062.1	0.0096	3.20	L	
<i>Enzymes</i>		ADP/ATP translocase 3	DAA33747.1	0.0410	2.11	L
		Alpha-1-antiproteinase	P34955.1	0.0039	2.81	NU
	Bovine Mitochondrial F1-Atpase	2W6F	0.0054	14.72	NU	
	Cathepsin C	AAI02116.1	0.0127	2.01	L	
	Fatty acyl-CoA reductase 2	DAA29455.1	0.0353	3.99	L	
	Precursor of Protein-lysine 6-oxidase	DAA27688.1	0.0164	6.13	L	
	Pyruvate Kinase 2	AAI02827.1	0.0107	2.08	NU	
	Isoform X2 of Serpin B6	XP_015315506.2	0.0004	10.37	NU	
	<i>Serum Proteins</i>	A Chain A, Bovine Fab E03 Light Chain	5IJV	0.0102	5.22	NU
Albumin		754920A	0.0415	6.26	NU	
Alpha-2-macroglobulin		Q7SIH1.2	0.0039	18.34	NU	
Isoform X1 of Complement component C8 gamma chain		XP_005213573.2	0.0012	2.44	L	
Precursor of Complement component C9		NP_001030441.1	0.0431	2.30	L	
Immunoglobulin J chain		AAB03643.1	0.0105	3.31	L	

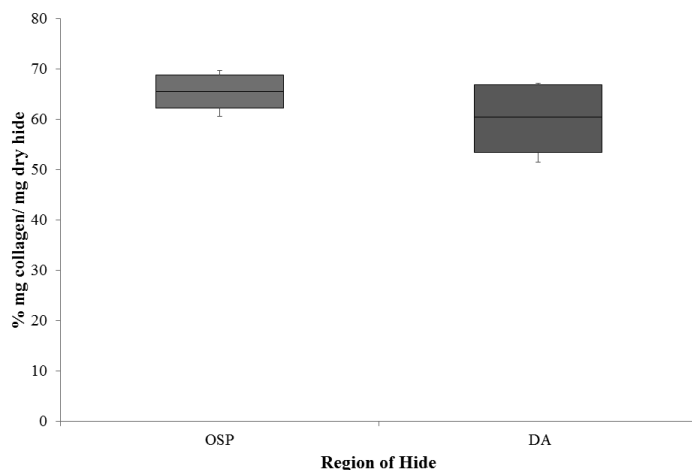


Figure 8. Collagen concentration of OSP and DA regions calculated from hydroxyproline concentration.

concentration of keratins could also be due to sampling issues. However, it must be noted that in cells of the dermis, keratin filaments and other intermediate filaments function as part of the cytoskeleton to mechanically stabilise the cell against physical stress. So, a decrease in these filaments could cause a less mechanically stable cell structure. Other cellular proteins that have a role in supporting the structure of dermal cells include annexin, tubulin and myosin.

Of the enzymes that were down-regulated in the DA region, protein-lysine-6-oxidase was of the most interest. It is an enzyme essential for the formation of crosslinks between tropocollagen molecules as well as various extracellular matrix proteins including elastin.⁴⁶ In humans, the lack of vitamin C, an essential cofactor of this enzyme, leads in the worst cases to scurvy, a disease first recorded in 1550 BCE whose symptoms are impaired wound healing and broken skin among others.⁴⁷ Down regulation of this enzyme would result in defective fibrillogenesis leading to the increased gaps and less organised structure of the collagen fibers seen in the DA samples (Fig 5). There was also a decrease in the lysosomal enzyme cathepsin C which activates serine proteases as well a decrease in the serine protease inhibitors alpha 1 anti-proteinase and isoform X2 of Serpin B6.

Conclusions

In this study, the DA region of the hide was used as a model for loose hide, with the OSP region being used as a control. Analysis of samples prepared using two different methods to extract the proteins showed advantages of this approach as it resulted in a more complete protein profile of hide than would have been achieved using a single method. Over 400 proteins were identified with high confidence and there were clear differences between the two regions tested some of which provided a molecular explanation for the differences in the collagen structure observed using confocal microscopy. It was particularly interesting that four of the proteins that were significantly down regulated in the DA are involved in or influence the arrangement of collagen microfibril bundles that are responsible for the physical properties of the hide. The decrease in these proteins are likely responsible for the increased gaps and less organised structure of the

collagen fibers seen with confocal microscopy. Although these results need to be validated, the preliminary studies indicate that there are molecular differences in the raw hides that produce loose and tight leather. Understanding the molecular causes of loose leather may enable biomarkers to be developed for its early detection.

Acknowledgements

This work was supported by NZ Leather and Shoe Research Association (LASRA[®]), Palmerston North, New Zealand through the Ministry of Business, Innovation and Employment (MBIE) grant numbers LSRX1301 and 1801 and 2019 IULTCS/ERRETRE/TFL Young Leather Scientist Grant. We would like to thank Massey University, Palmerston North, New Zealand for providing access to the Manawatu Microscopy and Imaging Centre and Mass Spectrometry Laboratory for acquiring the data. Dr. Torsten Kleffmann for his aid in analyzing the mass spectrometry data.

References

- Covington, A. D. *Tanning Chemistry: The Science of Leather*. Cambridge, UK: Royal Society of Chemistry, 2009.
- Sharphouse, J. H. *The Leatherworker's Handbook: Leather Producers' Association for England, Scotland and Wales*, 1963
- Annual Report 2018 - Meat Industry Association*. Retrieved from www.mia.co.nz, 2018.
- Wells, H. C., Holmes, G., & Haverkamp, R. G.; Looseness in bovine leather: microstructural characterization. *J. Sci. Food Agric*, **96** (8), 2751-2736, 2015.
- Wells, H. C., Holmes, G., & Haverkamp, R. G.; Early detection of looseness in bovine hides using ultrasonic imaging. *JALCA* **111**, 107-112, 2016.
- Liu, C. K., Laton, N. P., Lee, J., & Cooke, P. H.; Microscopic observations of leather looseness and its effects on mechanical properties. *JALCA* **104**, 230-236, 2009.
- Mehta, M., Naffa, R., Maidment, C., Holmes, G., & Waterland, M.; Raman and ATR-FTIR spectroscopy towards classification of wet blue bovine leather using ratiometric and chemometric analysis. *J. Soc. Leath. Sci. Eng.*, **2** (1), 3, 2020.
- Wood, B.; Looseness - Tanner's Dilemma. *Leather International*, **64**, 2000.
- Aslam, M., Khan, T. M., Naqvi, S. S., Holmes, G., & Naffa, R.; On the Application of Automated Machine Vision for Leather Defect Inspection and Grading: A Survey. *IEEE Access*, **7**, 176065-176086; 2019.
- Henrickson, R. L., Ranganayaki, M., Asghar, A., & Bailey, D. G.; Age, species, breed, sex, and nutrition effect on hide collagen. *Crit. Rev. Food Sci. Nutri*, **20** (3), 159-172, 1984.
- Naffa, R., Maidment, C., Ahn, M., Ingham, B., Hinkley, S., & Norris, G.; Molecular and structural insights into skin collagen reveals several factors that influence its architecture. *Int. J. Biol. Macromol*, **128**, 509-520, 2019.
- Naffa, R., Maidment, C., Holmes, G., & Norris, G. E.; Insights into the molecular composition of the skins and hides used in leather manufacture. *JALCA* **114**, 29-37, 2019.

13. Frantz, C., Stewart, K. M., & Weaver, V. M.; The extracellular matrix at a glance. *J. Cell Sci*, **123**, 4195-4200, 2010.
14. Mouw, J. K., Ou, G., & Weaver, V. M.; Extracellular matrix assembly: a multiscale deconstruction. *Nat. Rev*, **15**, 771-785, 2014.
15. Tobin, D. J.; Biochemistry of human skin - our brain on the outside. *Chem. Sci*, **35**, 52-67, 2006.
16. Fang, J., Wang, P., Huang, C., Chen, M., Wu, Y., & Pan, T.; Skin ageing caused by intrinsic or extrinsic processes characterize with functional proteomics. *Proteomics*, **16**, 2718-2731, 2016.
17. Randles, M. J., Humphries, M. J., & Lennon, R.; Proteomic definitions of basement membrane composition in health and disease. *Matrix biol*, **57**, 12-28, 2017.
18. Keller, U., Prudova, A., Eckhard, U., Fingleton, B., & Overall, C. M.; Systems-level analysis of proteolytic events in increased vascular permeability and complement activation in skin inflammation. *Sci. Signaling*, **6** (258), 1-14, 2013.
19. Lundberg, K. C., Fritz, Y., Johnston, A., Foster, A. M., Baliwag, J., Gudjonsson, J. E., Schlatzert, D., Gokulrangan, G., McCormick, T. S., Chancet, M. R., & Wards, N. L.; Proteomics of skin proteins in Psoriasis: From discovery and verification in a mouse model to confirmation in humans. *Protein Sci*, **14** (1), 109-119, 2015.
20. Boschetti, E., Hernández-Castellano, L. E., & Righetti, P. G.; Progress in farm animal proteomics: The contribution of combinatorial peptide ligand libraries. *Proteomics*, **197**, 1-13, 2019.
21. Singh, B., Mal, G., Gautam, S. K., & Mukesh, M.; Proteomics: Applications in Livestock. In *Advances in Animal Biotechnology* (pp. 387-395): Springer, 2019.
22. Choudhury, S. D., Allsop, T., Passman, A., & Norris, G.; Use of a proteomics approach to identify favourable conditions for production of good quality lambskin leather. *Anal. Bioanal. Chem*, **384** (3), 723-735, 2006.
23. Edmonds, R. L., Choudhury, S. D., Haverkamp, R. G., Britles, M., Allsop, T. F., & Norris, G. E.; Using Proteomics, Immunohistology, and Atomic Force Microscopy to Characterize Surface Damage to Lambskins Observed after Enzymatic Dewooling. *J. Agric. Food Chem*, **56**, 7934-7941, 2008.
24. Muthiah, P. L., Ramanathan, N., & Nayudamma, Y. Biochemical studies of the skin samples obtained from different sites on various animals. *JALCA* **63**, 38-47.
25. Rose, E. H., Vistnes, L. M., & Ksander, G. A.; A microarchitectural model of regional variations in hypodermal mobility in porcine and human skin. *Ann. Plast. Surg*, **1** (3), 252-266, 1978.
26. Oh, J., Byrd, A. L., Deming, C., Conlan, S., Barnabas, B., Blakesley, R., Bouffard, G., Brooks, S., Coleman, H., & Dekhtyar, M.; Biogeography and individuality shape function in the human skin metagenome. *Nature*, **514** (7520), 59-64, 2014.
27. Hinzke, T., Kouris, A., Hughes, R.-A., Strous, M., & Kleiner, M.; More is not always better: evaluation of 1D and 2D-LC-MS/MS methods for metaproteomics. *Front. Microbiol*, **10**, 238, 2019.
28. Byron, A., Humphries, J. D., & Humphries, M. J.; Defining the extracellular matrix using proteomics. *Int. J. Exp. Pathol*, **94**, 75-92, 2013.
29. Bian, Y., Zheng, R., Bayer, F. P., Wong, C., Chang, Y.-C., Meng, C., Zolg, D. P., Reinecke, M., Zecha, J., & Wiechmann, S.; Robust, reproducible and quantitative analysis of thousands of proteomes by micro-flow LC-MS/MS. *Nat. Commun*, **11** (1), 1-12, 2020.
30. Zakharchenko, O., Greenwood, C., Alldridge, L., & Souchelnyskiy, S.; Optimized protocol for protein extraction from the breast tissue that is compatible with two-dimensional gel electrophoresis. *Breast cancer*, **5**, 38-42, 2011.
31. Bradford, M. M.; A rapid and sensitive method for the quantitation of microgram quantities of protein utilizing the principle of protein-dye binding. *Anal. biochem*, **72** (1), 248-254., 1976
32. Laemmli, U. K.; Cleavage of structural proteins during the assembly of the head of bacteriophage T4. *Nature*, **227** (5259), 680-685, 1970.
33. Shevchenko, A., Tomas, H., Havli, J., Olsen, J. V., & Mann, M.; In-gel digestion for mass spectrometric characterization of proteins and proteomes. *Nat. prot*, **1** (6), 2856, 2006.
34. Vogel, B., Siebert, H., Hofmann, U., & Frantz, S.; Determination of collagen content within picosirius red stained paraffin-embedded tissue sections using fluorescence microscopy. *MethodsX*, **2**, 124-134, 2015.
35. Switzar, L., Giera, M., & Niessen, W. M.; Protein digestion: an overview of the available techniques and recent developments. *J. Proteome Res*, **12** (3), 1067-1077, 2013.
36. Jiang, X., Jiang, X., Feng, S., Tian, R., Ye, M., & Zou, H.; Development of efficient protein extraction methods for shotgun proteome analysis of formalin-fixed tissues. *J. Proteome Res*, **6** (3), 1038-1047, 2007.
37. Sheoran, I. S., Ross, A. R., Olson, D. J., & Sawhney, V. K.; Compatibility of plant protein extraction methods with mass spectrometry for proteome analysis. *Plant Sci*, **176** (1), 99-104, 2009.
38. Prusa, K. J., & Bowers, J. A.; Protein extraction from frozen, thawed turkey muscle with sodium nitrite, sodium chloride, and selected sodium phosphate salts. *J. Food Sci*, **49** (3), 709-713, 1984.
39. Swaney, D. L., Wenger, C. D., & Coon, J. J.; Value of using multiple proteases for large-scale mass spectrometry-based proteomics. *J. Proteome Res*, **9** (3), 1323-1329, 2010.
40. Gelse, K., Poschl, E., & Aigner, T.; Collagen - structure, function, and biosynthesis. *Adv. Drug Deliv. Rev*, **55**, 1531-1546, 2003.
41. Ricard-Blum, S.; The collagen family. *Cold Spring Harb. Perspec. biol*, **3** (1), 1-19, 2011.
42. Neuman, R. E., & Logan, M. A.; The determination of hydroxyproline. *J. Biol. Chem*, **184**, 299-306, 1950.
43. Li, Y., Liu, Y., Xia, W., Lei, D., Voorhees, J. J., & Fisher, G. J.; Age-dependent alterations of decorin glycosaminoglycans in human skin. *Sci Rep*, **3** (2422), 1-8, 2013.
44. Perides, G., Asher, R., Lark, M., Lane, W., Robinson, R., & Bignami, A.; Glial hyaluronate-binding protein: a product of metalloproteinase digestion of versican? *Biochem. J*, **312** (2), 377-384, 1995.
45. Schaefer, L., & Schaefer, R. M.; Proteoglycans: from structural compounds to signaling molecules. *Cell Tissue Res*, **339** (1), 237-246, 2009.
46. Rucker, R. B., Kosonen, T., Clegg, M. S., Mitchell, A. E., Rucker, B. R., Uriu-Hare, J. Y., & Keen, C. L.; Copper, lysyl oxidase, and extracellular matrix protein cross-linking. *American J. Clin. Nutr*, **67** (5), 996S-1002S, 1998.
47. Pritzker, K. P., & Kessler, M. J.; Arthritis, muscle, adipose tissue, and bone diseases of nonhuman primates. In *Nonhuman primates in biomedical research* (pp. 629-697): Elsevier, 2012.